

Pre- and Post-Sexual Maturity Liver-specific ER α Knockout Does Not Impact Hepatic Mitochondrial Function

Kelly N. Z. Fuller,^{1,2} Julie Allen,^{1,2} Roshan Kumari,^{1,2} Jephthe Y. Akakpo,³ Meghan Ruebel,⁴ Kartik Shankar,⁴ and John P. Thyfault^{1,2,5,6,7}

¹Department of Cell Biology and Physiology, University of Kansas Medical Center, Kansas City, KS 66160, USA

²Research Service, Kansas City Veterans Affairs Medical Center, Kansas City, KS 64128, USA

³Department of Pharmacology and Toxicology, University of Kansas Medical Center, Kansas City, KS 66160, USA

⁴USDA-ARS, Southeast Area, Arkansas Children's Nutrition Center, Little Rock, AR 72202, USA

⁵KU Diabetes Institute and Kansas Center for Metabolism and Obesity, University of Kansas Medical Center, Kansas City, KS 66160, USA

⁶Department of Internal Medicine, Division of Endocrinology and Metabolism, University of Kansas Medical Center, Kansas City, KS 66160, USA

⁷Center for Children's Healthy Lifestyles and Nutrition, Kansas City, MO 64108, USA

Correspondence: John P. Thyfault, PhD, Professor, Director, and Senior Research Scientist, Hemenway Life Sciences Innovation Center, University of Kansas Medical Center, Mailstop 3043, 3901 Rainbow Boulevard, Kansas City, KS 66160, USA. Email: jthyfault@kumcd.edu.

Abstract

Compared with males, premenopausal women and female rodents are protected against hepatic steatosis and present with higher functioning mitochondria (greater hepatic mitochondrial respiration and reduced H₂O₂ emission). Despite evidence that estrogen action mediates female protection against steatosis, mechanisms remain unknown. Here we validated a mouse model with inducible reduction of liver estrogen receptor alpha (ER α) (LERKO) via adeno-associated virus (AAV) Cre. We phenotyped the liver health and mitochondrial function of LERKO mice (n = 10–12 per group) on a short-term high-fat diet (HFD), and then tested whether timing of LERKO induction at 2 timepoints (sexually immature: 4 weeks old [n = 11 per group] vs sexually mature: 8–10 weeks old [n = 8 per group]) would impact HFD-induced outcomes. We opted for an inducible LERKO model due to known estrogen-mediated developmental programming, and we reported both receptor and tissue specificity with our model. Control mice were ER α ^{fl/fl} receiving AAV with green fluorescent protein (GFP) only. Results show that there were no differences in body weight/composition or hepatic steatosis in LERKO mice with either short-term (4-week) or chronic (8-week) high-fat feeding. Similarly, LERKO genotype nor timing of LERKO induction (pre vs post sexual maturity) did not alter hepatic mitochondrial O₂ and H₂O₂ flux, coupling, or OXPHOS protein. Transcriptomic analysis showed that hepatic gene expression in LERKO was significantly influenced by developmental stage. Together, these studies suggest that hepatic ER α is not required in female protection against HFD-induced hepatic steatosis nor does it mediate sexual dimorphism in liver mitochondria function.

Key Words: estrogen, sex hormones, fatty liver, metabolism

Abbreviations: 4HNE, 4-hydroxynonenal; AAV, adeno-associated virus; CDCA, chenodeoxycholic acid; CON, control; DEG, differentially expressed gene; ECM, extracellular matrix; ER α , estrogen receptor alpha; GFP, green fluorescent protein; GPER, G-protein coupled estrogen receptor; HFD, high-fat diet; IM, sexually immature; KO, knockout; LC-MS/MS, liquid chromatography–tandem mass spectrometry; LERKO, liver-specific estrogen receptor alpha knockout; LFD, low-fat diet; MAT, sexually mature; MCA, muricholic acid; NAFLD, nonalcoholic fatty liver disease; PCR, polymerase chain reaction; ROS, reactive oxygen species; SEM, standard error of the mean.

Loss of estrogen action is associated with many metabolic diseases, including obesity, type 2 diabetes [1], metabolic syndrome [2], and nonalcoholic fatty liver disease (NAFLD) [3]. This strong relationship arises from the fact that estrogen plays critical and diverse roles in metabolism (energy balance, insulin sensitivity, fat metabolism, mitochondrial function, inflammation, etc) across a variety of tissues [4]. With particular focus on the liver, premenopausal women [5, 6] and intact female rodents [7] are protected from diet-induced steatosis, which is lost during estrogen withdrawal via menopause or ovariectomy but restored with estrogen treatment [8]. Given that rates of hepatic steatosis (greater than 5% of liver weight comprising lipids) are rising and NAFLD is now the leading type of liver

disease in the United States [9], understanding the mechanisms of estrogen-driven hepatic protection is both timely and critical.

Emerging work from our group and others suggest a sexual dimorphism in hepatic mitochondrial function in response to metabolic stressors (high-fat diet, exercise, etc) where females appear to have better coupled mitochondria with lower reactive oxygen species emission compared with males [7, 10, 11]. These results appear dependent on estrogen and track well with risk of developing steatosis [12]. Evidence of early mitochondrial abnormalities in NAFLD includes decreased mitochondrial DNA [13], enlarged and swelled mitochondria [14], and reduced hepatic fatty acid oxidation [15]. As NAFLD progresses from steatosis to steatohepatitis

(NASH), further morphological and functional changes in hepatic mitochondria can be observed, such as loss of cristae and paracrystalline inclusions [16], lower respiratory chain complex activity [17], and reduced rates of mitochondrial respiration [18]. These data from both human and rodent work not only suggest that mitochondria may be an important factor in NAFLD pathophysiology but may also be an underlying mechanism of the sex differences seen in NAFLD. Data from ChIP Seq studies have found that hepatic estrogen receptor alpha (ER α) mediates lipid metabolism, TCA cycle genes, and mitochondrial electron transport system proteins [19], outlining a possible link between estrogen action, liver mitochondria, and NAFLD sexual dimorphism. Despite this, much of the literature surrounding estrogen, ER α , and steatosis risk remains focused on systemic insulin resistance [20], triglyceride handling and export in the liver [8], and regulation of lipolysis in adipose tissue [21]. Over recent years, there has been a large effort focused on understanding estrogen's regulation of mitochondrial function via ER α signaling in skeletal muscle [22, 23]; however, much less is known about ER α signaling and mitochondrial function in the liver.

Estrogen action is primarily mediated by ER α and ER β as well as cell surface G-protein coupled estrogen receptors (GPER) [24]. In the liver, the major form of regulation occurs via genomic signaling, where estrogen binding to ER initiates downstream regulation of estrogen response elements (EREs) in the nucleus. While both ER α and GPER are present in the mouse liver [25], ER α is the dominant receptor [26]. The importance of ER α in female prevention against steatosis has been previously investigated with use of transgenic animal models. Hart-Unger et al reported that on a high-fat diet (HFD), female global ER α knockout mice and ER α DNA-binding domain mutant mice develop hepatic steatosis, but liver-specific ER α knockout (LERKO) mice do not [27], suggesting that steatosis is mediated by ER α -driven direct transcription in extrahepatic tissues. However, other groups suggest that LERKO abolishes the ability of estradiol treatment to prevent steatosis following ovariectomy [28]. This occurs despite maintained estradiol-driven reductions in whole body metabolic outcomes such as body weight and adiposity [8], suggesting protective hepatic-specific mechanisms of ER α . These and the majority of other existing reports in LERKO mice have employed conventional knockout models (breeding ER $\alpha^{fl/fl}$ mice with albumin Cre mice), resulting in liver-specific deletion of ER α during embryonic development, a potential confounder and inducer of compensatory adaptations, as estrogen is known to have many critical roles during this period [29]. Moreover, we are not aware of studies that have phenotyped hepatic mitochondrial respiratory function or reactive oxygen species in the context of hepatic-specific deletion of ER α .

Given that the role of hepatic ER α in female protection against steatosis and its association with mitochondrial function remains incompletely understood, this present study aimed to investigate this question along with potential underlying mechanisms with use of an inducible LERKO model that preserves hepatic ER α function until experimental reduction by in vivo adeno-associated virus (AAV) Cre injection. We hypothesized that conditional liver-specific knockout of ER α (LERKO) would perturb hepatic mitochondrial function toward lower maximal respiration and coupling, increasing H₂O₂ emission and steatosis susceptibility. Given the surge of estrogen that occurs during sexual puberty [30] and the

potential for a priming effect that possibly programs long-term metabolic and mitochondrial programming in the liver, we also hypothesized that induction of LERKO at sexual immaturity would cause a more pronounced phenotype compared to induction of LERKO post sexual maturity.

Materials and Methods

Ethical Approval

All animal protocols were approved by the Institutional Animal Care and Use Committee at the University of Kansas Medical Center and Kansas City VA Medical Center (Protocol #s 2018-2456, 2019-2539). Experiments were completed in accordance with the Guide for the Care and Use of Laboratory Animals published by the US National Institutes of Health. Mice were anesthetized with phenobarbital (0.5 mg/g BW) before terminal procedures following a 2-hour fast in the light cycle (7:00-9:00).

Animals

Only female mice were used in these studies to focus on whether the enhanced mitochondrial function and protection against hepatic steatosis found in female mice is dependent on ER α . The liver-specific ER α knockout (LERKO) mice (provided by Dr. Mark Johnson at University of Missouri Kansas City, obtained with permission from Dr. Stavros Manolagas at University of Arkansas for Medical Sciences) used in these studies have been described previously [31]. For these present studies, male and female ER α homozygous floxed (ER $\alpha^{fl/fl}$) mice on a C57Bl/6 background were bred together resulting in ER $\alpha^{fl/fl}$ mice and identified by polymerase chain reaction (PCR)-based genotyping of tail snips. ER $\alpha^{fl/fl}$ mice were injected with one of two adeno-associated viruses (Addgene, Watertown, MA): AAV Cre (AAV.TBG.PI.Cre.rBG) to specifically delete ER α in the liver (LERKO) or with an AAV that only expresses green fluorescent protein (GFP) (pAAV.TBG.PI.eGFP.WPRE.bGH) and does not delete the floxed region (Control). Both injections were delivered as 200 μ L intraperitoneal injection diluted in saline to 1.5¹¹ GC per mouse.

Mice were singly housed at thermoneutral temperatures (~30 °C) on a reverse light cycle (dark 10:00-22:00) with ad libitum access to water and low-fat diet (LFD; Research Diets D12110704: 10% kcal fat, 3.5% kcal sucrose, 3.9 kcal/g) or high-fat diet (HFD; Research Diets D12451: 45% kcal fat, 17% kcal sucrose; 4.7 kcal/g) for the entirety of the studies.

Experimental Design

Our first experiment aimed to validate the tissue- and receptor specificity of the LERKO model. Male and female ER $\alpha^{fl/fl}$ mice were injected with AAV Cre or AAV GFP at 4 months of age, generating n = 4 mice per group. Mice were fed LFD and sacrificed 2 weeks after injection.

Our second experiment aimed to phenotype liver mitochondrial function (respiration, H₂O₂ emission, coupling) in female LERKO (AAV Cre) and control (AAV GFP) ER $\alpha^{fl/fl}$ mice under short-term metabolic challenge via high-fat diet (HFD). Mice (n = 10-12 per group) were singly housed and placed on HFD 1 to 3 days prior to injection. Mice remained on HFD for 4 weeks until sacrifice (41-42 days postinjection). At injection, mice were between 2 and 7.5 months of age. Given the results from our first experiment, we considered 2

weeks postinjection full induction of the desired genotype, marking day 1 of the rest of the intervention and baseline “pre” for body composition measures.

Our third experiment largely followed the same experimental design as Experiment 2 (Fig. 1) and aimed to determine whether timing of Cre injection and subsequent induction of LERKO genotype (sexual immaturity vs sexual maturity) impacted hepatic mitochondrial outcomes and steatosis. For this experiment, animals were singly housed and placed on HFD 2 to 4 days prior to injection which occurred at 4 weeks and 8 to 10 weeks of age, respectively, for sexual immature (IM) and mature (MAT) animals ($n = 8-11$ per group). Duration of the HFD was 8 weeks following genotype induction, twice the length utilized in Experiment 2.

For both Experiment 2 and 3, a small subset of mice ($n = 1-2$ per genotype) were sacrificed 2 weeks postinjection to confirm LERKO induction via RT-PCR.

Anthropometrics

Body weight was measured weekly throughout the studies and body composition was measured at the beginning and end of each study via magnetic resonance imaging (EchoMRI, Houston, TX). Food intake was measured twice per week and HFD was replaced at the same interval to prevent rancidification. At sacrifice, whole blood was collected via cardiac puncture and centrifuged (4 °C, 10 minutes, 7000g) for serum separation following clotting at room temperature cooling on ice for 10 minutes. Serum triglycerides were measured with a commercially available kit (Sigma-Aldrich, St. Louis, MO).

Hepatic Mitochondrial Isolation, Respiration, and H₂O₂ Flux

Hepatic mitochondrial isolation was performed as described previously [7, 10, 11]. Briefly, livers were quickly excised and submerged in 8 mL cold mitochondrial isolation buffer (220 mM mannitol, 70 mM sucrose, 10 mM Tris, 1 mM EDTA, pH 7.4) and homogenized on ice with a Teflon pestle. Homogenates were centrifuged (4 °C, 10 minutes, 1500g), strained through gauze, and the supernatant was centrifuged again (4 °C, 10 minutes, 8000g). The supernatant was discarded and the resulting mitochondrial pellet was resuspended with 6 mL mitochondrial isolation buffer via 3 to 4 passes of glass-on-glass homogenization, before centrifugation (4 °C, 10 minutes, 6000g). The process was repeated, using 4 mL mitochondrial isolation buffer with the addition of 0.1% fatty acid-free BSA and lower centrifugation speed (4 °C, 10 minutes, 6000g). The final mitochondrial pellet was resuspended in 300 to 500 μ L modified MiRO5 mitochondrial respiration buffer (0.5 mM EGTA, 3 mM MgCl₂, 60 mM KMES,

20 mM glucose, 10 mM KH₂PO₄, 20 mM HEPES, 110 mM sucrose, 0.1% BSA, pH 7.1) and used in mitochondrial respiration studies.

Mitochondrial respiration and H₂O₂ flux were measured simultaneously using the Oroboros O2k-FluoRespirometer (O2k, Oroboros Instruments, Austria) as previously outlined [7, 10, 11]. Calibration was performed daily, and chamber conditions were kept constant (30 °C, 750 rpm stir speed, chamber lights off). Mitochondrial experiments were performed with starting substrates of 2 mM malate, 10 μ M coenzyme A, and 2.5 mM L-carnitine and then either potassium-pyruvate (PYR; 5 mM) or palmitoyl-coenzyme A (PCoA; 10 μ M) to assess potential substrate differences. Once steady state basal respiration was established, subsequent injections were made to capture maximal respiratory flux at different respiratory states: 2.5 mM adenosine 5'-diphosphate (ADP; State 3), 10 mM succinate (Succ; State 3S), and 0.005 μ M carbonyl cyanide-p-trifluoromethoxyphenyl hydrazone (FCCP; Uncoupled) injections until maximum. All outcomes were analyzed with DatLab 7 (Oroboros Instruments, Austria) and normalized to both volume of mitochondrial isolate added to the O2k chamber and total protein in the isolate determined via bicinchoninic acid protein assay (ThermoFisher Scientific, Waltham, MA). Coupling control ratio was calculated as basal respiration/state 3 respiration to infer mitochondrial coupling [32]. H₂O₂:O₂ ratios were calculated as H₂O₂ flux/O₂ flux to evaluate relative H₂O₂ production at different respiratory states.

Liver Triglycerides

As done previously [10], lipid was extracted from 25 to 30 mg of flash frozen liver tissue and reconstituted in a tert-butanol-Triton X solution before determining liver triglyceride content via a commercially available kit (Sigma-Aldrich, St. Louis, MO). Concentrations are reported as mg/g of total liver tissue used in the assay. For this outcome, as well as others described below, several liver lobes were smashed and powdered together via pestle and mortar in liquid nitrogen. This technique is expected to capture the heterogeneity of the liver. In addition, liver was fixed in formalin, embedded in paraffin, and prepared for hematoxylin and eosin (H&E) staining.

Western Blotting

Roughly 75 mg of flash frozen liver tissue was homogenized in homogenization buffer (50 mM HEPES, 12 mM sodium pyrophosphate, 100 mM sodium fluoride, 10 mM EDTA), with phosphatase inhibitors (Phosphatase Inhibitor Cocktail 2 and 3; Sigma-Aldrich, St. Louis, MO), protease inhibitors (EDTA-free Protease Inhibitor Cocktail; Roche Diagnostics, Germany), and 1% Triton X-100 using the TissueLyzer II

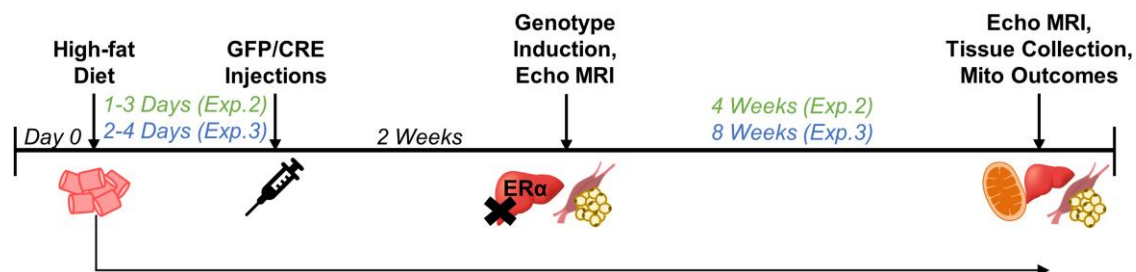


Figure 1. Experimental design.

(Qiagen, Germantown, MD). Whole liver homogenate Western-ready Laemmli samples were separated with SDS-PAGE, transferred to a polyvinylidene difluoride membrane, and blocked overnight at 4 °C in a 5% milk TBST solution. Following several rounds of washing with TBST at room temperature, membranes were incubated at 4 °C overnight with primary antibody at 1:2000 concentration for ER α (ab32063), ER β (ab288), total OXPHOS (ab110413), and 4-hydroxynonenal (4HNE, ab46545). Membranes were then incubated in the appropriate secondary antibody solution at 1:10 000 concentration for an hour at room temperature. All primary antibodies were purchased from Abcam (Cambridge, MA) and secondary antibodies were from Cell Signaling Technology (Danvers, MA). Membranes were imaged and densitometry performed for quantification of protein bands using Image Laboratory software (Bio-Rad Laboratories, Hercules, CA). All Western blot data was normalized to total protein stain with 0.1% amido black.

RNA Sequencing

RNA sequencing was performed in immature and mature AAV Cre mice studies (Experiment 3). RNA was extracted from liver tissue using the RNeasy Mini Kit (Qiagen, Germantown, MD) per manufacturer's instructions. Isolated RNA from liver was cleaned with the QIAamp RNA Blood Mini Kit (52304) according to the standard protocol. The cleaned RNA was quantified using a Qubit RNA BR Assay Kit (ThermoFisher, Q10210) and the RIN was assessed on an RNA ScreenTape (Agilent, Cat. No. 5067-5577 and 5067-5576) on the TapeStation platform prior to library preparation. RNA libraries were prepared using a TruSeq Stranded RNA HT Sample Prep Kit (Illumina, Cat. No. RS-122-2303) on a Caliper (now Perkin Elmer) Sciclone G3 platform. An additional standard 1.0 \times manual bead cleanup was performed using AMPure XP Beads (Beckman Coulter, A63881) after the libraries were completed to clean up primer-dimers. Qubit dsDNA BR Assay kit was used to determine the concentration of the completed library and a Fragment Analyzer Standard Sensitivity NGS Fragment Kit (Agilent, Cat. No. DNF-473-10000) was used to detect the size of the library and to verify removal of excess primer-dimers. Standard Illumina Free-Adapter Blocking was performed on the completed libraries. Cleaned, adapter-blocked libraries were loaded on a NovaSeq6000 with a run configuration of 151 \times 8 \times 8 \times 151 and an average depth of 84 M PE reads per library.

RNA-seq Data Analyses

Following sequencing and demultiplexing, all reads were trimmed for adapters, filtered based on quality score, and aligned to the mouse genome (mm10) using the STAR aligner. Resulting read alignments for each sample were imported in Seqmonk for gene level quantification as counts mapping to annotated genes. Gene counts were imported into R (v4.05) and analysis of differential expression between groups was

done using the limma-voom pipeline [33]. Transcripts with expression below 1 count/million were excluded from further analysis. Differentially expressed genes between 2 pair-wise comparisons (LERKO vs CON in immature mice; and LERKO vs CON in mature mice) were identified with an unadjusted *P* value <.05 and a minimum fold change \pm 1.5 fold. Further interpretive analysis of differentially expressed genes for enrichment of gene ontology (GO) terms was done using Enrichr [34], Ingenuity Pathway Analysis (Qiagen) and HumanBase functional module detection [35]. The HumanBase functional module analysis, utilizes tissue-specific network-based functional interpretation of gene lists, and applies community detection to find cohesive gene clusters from a provided gene list (<https://hb.flatironinstitute.org/module/>). Heatmaps and other plots were generated using packages in R.

mRNA Gene Expression

RNA extraction, cDNA preparation, and RT-PCR were performed as previously described. Briefly, RNA was extracted from liver tissue using the RNeasy Mini Kit (Qiagen, Germantown, MD) per manufacturer's instructions. The cDNA was prepared using the ImProm-II reverse transcription system (Promega, Madison, WI) and diluted to 10 ng/uL. SYBR green mouse primers (Sigma-Aldrich, St. Louis, MO; Table 1) were used for RT-PCR on a QuantStudio 3 (Thermo Fisher Scientific, Waltham, MA). Delta-delta Ct method was used to calculate relative fold gene expression normalized to the housekeeping gene Cyclophilin B (PPIB).

Liquid Chromatography–Tandem Mass Spectrometry Determination of Bile Acids

Liquid chromatography–tandem mass spectrometry (LC-MS/MS) analysis of bile acid (BA) metabolites in liver tissue was performed as described by Alnouti et al [36]. Briefly, 50 mg of liver tissue was homogenized in RIPA buffer. Blank matrix was prepared by stripping liver homogenate of endogenous bile acids. Activated charcoal (100 mg/mL) was mixed with control liver homogenate at maximum speed for 1 hour at room temperature in Eppendorf Thermomixer. Samples were centrifuged at 13 000g for 10 minutes and filtered through a 0.22 μ m cellulose filter. Then, 50 μ L of working standards were mixed with 50 μ L of stripped homogenate, 25 μ L of a solution containing bile acids internal standards, and methanol to make up the final volume of 500 μ L. Samples were vortexed for 10 seconds, chilled on ice for 10 minutes, centrifuged at 12 000g for 10 minutes at room temperature, lyophilized, and resuspended in 50 μ L of 1:1 methanol:water.

Samples analysis with LC-MS/MS was performed using a Waters Acquity Ultra-Performance Liquid Chromatography (UPLC) I-Class PLUS system interfaced by electrospray ionization with a Waters Xevo Triple quadrupole XS mass spectrometer (Waters Corp., Milford, MA) operated in negative mode with multiple reaction monitoring (MRM) scan type. The following source conditions were applied: 1.8 kV for

Table 1. RT-PCR primer sequences

Gene	Forward Primer	Reverse Primer
ESR1	CAAGGTAAATGTGTGGAAGG	GTGTACACTCCGGAATTAAG
ESR2	CTCAACTCCAGTATGTACCC	CATGAGAAAGAAGCATCAGG

Table 2. Anthropometrics

Variable (units)	CONTROL		LERKO	
<i>Experiment 1:</i>	n = 4		n = 4	
Body Weight Pre (g)	25.88 ± 1.90		27.00 ± 2.07	
Body Weight Post (g)	25.58 ± 2.23		26.80 ± 2.54	
Body Weight Change (g)	−0.30 ± 0.82		−0.20 ± 1.05	
Fat Mass Change (g)	0.53 ± 0.70		1.33 ± 0.62	
Fat-Free Mass Change (g)	−0.95 ± 0.89		−1.12 ± 0.51	
<i>Experiment 2:</i>	n = 10		n = 12	
Body Weight Pre (g)	23.91 ± 1.29		24.04 ± 1.23	
Body Weight Post (g)	25.66 ± 1.70		26.53 ± 1.71	
Body Weight Change (g)	1.75 ± 0.65		2.48 ± 0.94	
Fat Mass Change (g)	1.69 ± 0.61		1.47 ± 0.72	
Fat-Free Mass Change (g)	−0.17 ± 0.21		−0.28 ± 0.33	
Average Weekly Energy Intake (kcal)	62.96 ± 3.04		62.74 ± 3.03	
<i>Experiment 3:</i>	IM (n = 11)	MAT (n = 8)	IM (n = 11)	MAT (n = 8)
Body Weight Pre (g)	17.03 ± 0.93	19.81 ± 0.83	17.35 ± 0.43	19.64 ± 0.63
Body Weight Post (g)	21.93 ± 1.02	24.15 ± 2.29	22.45 ± 1.39	22.39 ± 1.10
Body Weight Change (g)	4.90 ± 0.73	4.44 ± 1.70	5.09 ± 1.07	2.75 ± 0.96
Fat Mass Change (g)	2.41 ± 0.68	2.94 ± 1.17	3.00 ± 1.10	2.19 ± 0.99
Fat-Free Mass Change (g)	3.43 ± 0.26	1.60 ± 0.11	3.17 ± 0.14	1.44 ± 0.24
Average Weekly Energy Intake (kcal)	53.07 ± 0.80	56.24 ± 2.20	55.92 ± 1.57	56.11 ± 2.17
Serum Triglycerides (mg/dL)	20.74 ± 2.23	29.58 ± 3.67	21.34 ± 2.13	20.93 ± 2.60

Values presented as mean ± SEM.

the capillary voltage, 150 °C for the source temperature, 500 °C for the desolvation temperature, and 1000 L/h for the desolvation gas flow. All metabolites were quantified by back calculation of a weighted (1/x), linear least squares regression. Samples above the calibration curve were further diluted 100-fold.

Statistical Analyses

Statistical analyses were performed with SPSS Statistics 27 (IBM, Armonk, NY). First, outliers were identified using the ROUT method with Prism (GraphPad Software, San Diego, CA) and excluded from analysis. Differences between CON vs LERKO were assessed via an independent T-test. For Experiment 3, all statistical analyses are within cohort (IM, MAT) although data are presented on the same graph. Significance was $P < .05$ and data are reported as mean ± standard error of the mean (SEM). After first separating Experiment 1 data by sex and showing no differences, we opted to combine male and female animals for greater sample size. Experiments 2 and 3 only utilized female mice.

Results

Anthropometric Measures Did Not Differ Between Control and LERKO Mice

Body weight, fat mass, and fat-free mass change (post-pre) over the course of the HFD intervention was similar between control and LERKO groups in all 3 experiments (Table 2). Energy intake was evaluated during Experiments 2 and 3 and did not differ by genotype. Serum triglycerides were also statistically similar

between CON and LERKO females in Experiment 3, although the MAT CON animals tended to have elevated levels compared to MAT LERKO animals ($P = .08$).

Experiment 1. The Inducible LERKO Model Is Specific to ER α in the Liver and Does Not Alter Liver TG Content.

We validated the receptor- and tissue- specificity of the inducible LERKO mouse model with RT-PCR and Western blotting. AAV Cre (LERKO) resulted in significantly lower liver ESR1 mRNA gene expression ($P < .05$; Fig. 2A) compared to the AAV only expressing GFP (CON). As expected, ESR2 mRNA gene expression was below detectable limits in the liver. LERKO animals also presented with ~58% lower liver ER α protein compared to controls ($P = .001$; Fig. 2B), with no differences in liver ER β protein expression between groups, confirming receptor specificity (Fig. 2C). ER α protein levels from mixed gastrocnemius skeletal muscle were equal between groups (Fig. 2D), confirming tissue specificity.

It has previously been established that estrogen action is required for protection against hepatic steatosis in intact female mice, leading us to investigate liver triglyceride content through a quantitative assay. Not surprisingly, we did not see any differences in liver triglycerides between control and LERKO mice fed a LFD (Fig. 2E). Given our validated LERKO model, we were next interested in evaluating steatosis and mitochondrial outcomes in the context of a HFD (Experiments 2, 3).

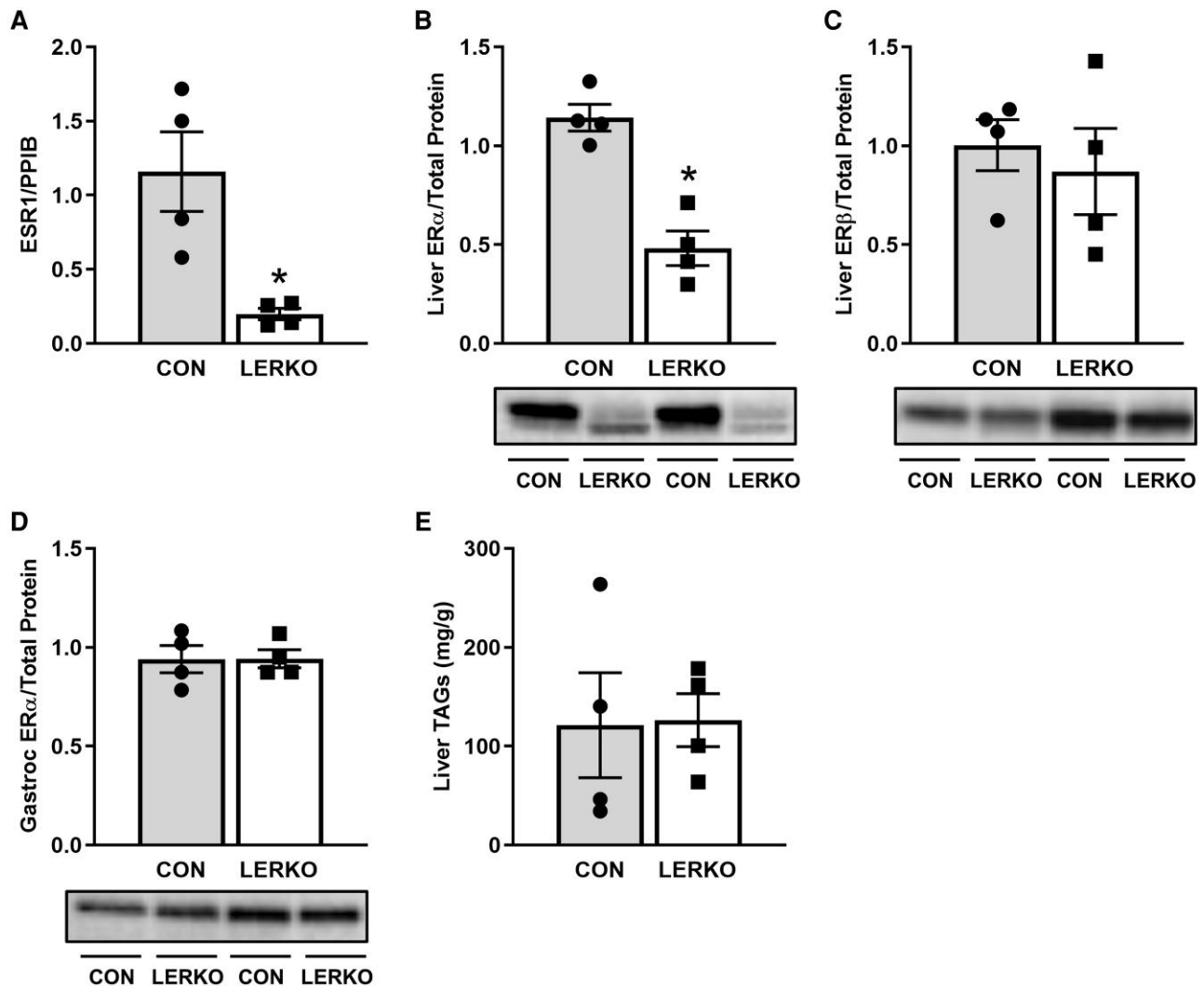


Figure 2. AAV Cre successfully induced the LERKO genotype in $ER\alpha^{fl/fl}$ mice. mRNA gene expression for liver ESR1 (A) was determined with RT-PCR. Protein expression of $ER\alpha$ (B: liver, D: gastrocnemius) and $ER\beta$ (C: liver) was determined via Western blotting and normalized to total protein using amido black staining. Liver triglyceride content (E) was quantified via biochemical assay. Data are presented as mean \pm SEM; $n = 4$ per group; all mice were fed a low-fat diet and singly housed at thermoneutral; *denotes a significant difference ($P < .05$) compared with control animals.

Experiment 2. LERKO Mice Do Not Have Greater Liver Triglycerides

We first confirmed our inducible knockout (KO) using RT-PCR and found a statistically significant difference (69% lower) in mRNA expression of $ER\alpha$ in LERKO mice compared with Controls ($P < .01$; Fig. 3A). Given strong evidence that estrogen is protective against hepatic steatosis in women, we wanted to evaluate whether liver $ER\alpha$ plays a role in this protection. Here we show no difference in hepatic steatosis measured via biochemical assay between CON and LERKO mice fed an acute HFD (Fig. 3B).

Experiment 2. Liver Mitochondrial Measures Were Similar in Female Control and LERKO Mice

We wanted to determine if deletion of liver $ER\alpha$ would change hepatic mitochondrial function in female mice. LERKO mice did not differ in hepatic mitochondrial respiration or H_2O_2 emission under either pyruvate or palmitoyl-CoA substrate conditions compared with controls (Fig. 4A-4D). Hepatic whole homogenate protein expression

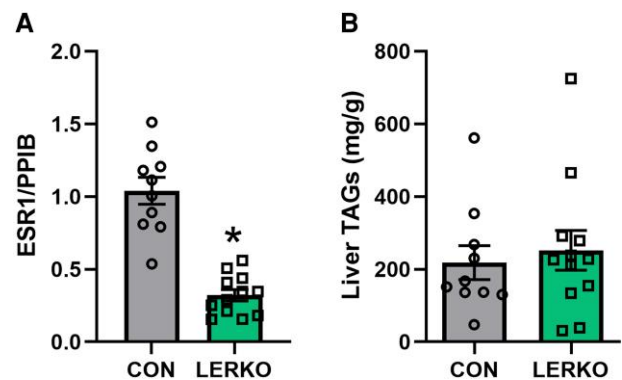


Figure 3. Hepatic $ER\alpha$ mRNA levels, but not triglyceride content, differ between CON and LERKO mice. ESR1 mRNA gene expression was determined with RT-PCR and normalized to PPIB (A). To capture steatosis, liver triglycerides (B) were measured via a biochemical assay. Data are presented as mean \pm SEM; $n = 10-12$ per group; all mice were fed an acute high-fat diet (4 weeks) and singly housed at thermoneutral; *denotes a significant difference ($P < .01$) compared with control animals.

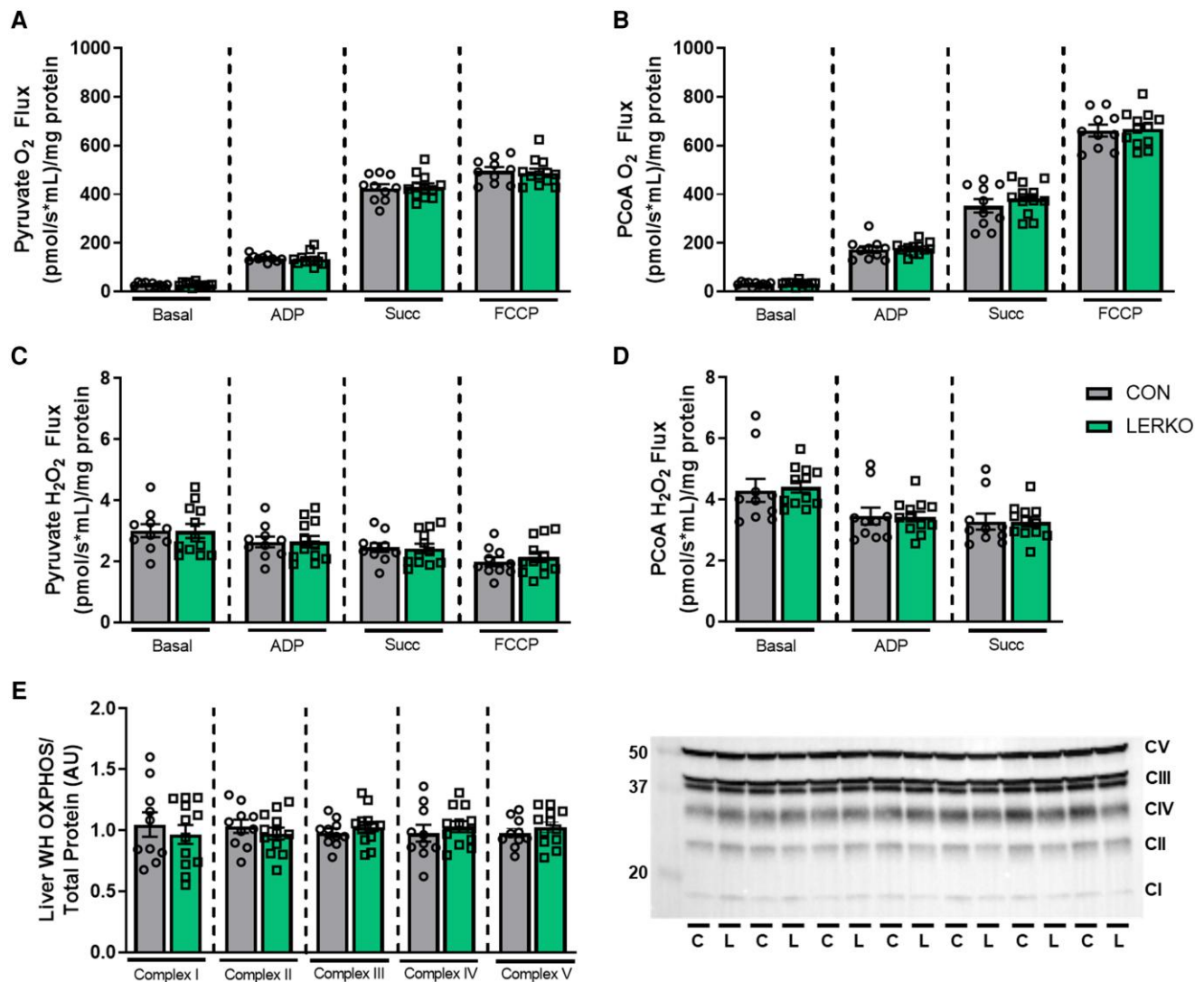


Figure 4. Hepatic mitochondrial respiration, H₂O₂, and OXPHOS protein were similar between CON and LERKO animals. Mitochondrial respiratory capacity (A, B) and H₂O₂ (C, D) were simultaneously measured in isolated liver mitochondria with an O₂k-Fluorometer. Measures were made under either pyruvate or palmitoyl-CoA (PCoA) substrate conditions. All data were normalized to total protein in the mitochondrial isolate measured via BCA assay. OXPHOS protein complexes were determined via Western blotting and normalized to total protein using amido black staining (E). A representative immunoblot is shown where C denotes the control animal, and L denotes LERKO. Data are presented as mean \pm SEM; n = 10-12 per group; all mice were fed an acute high-fat diet (4 weeks) and singly housed at thermoneutral. Statistical differences across mitochondrial respiratory states were not determined.

levels of the oxidative phosphorylation complexes (OXPHOS) were also not different between Control and LERKO mice (Fig. 4E).

Experiment 3. Ten Weeks Following Injection, LERKO mRNA Profile Remains Altered but Liver Protein Levels Mirror Control Animals

We chose to utilize inducible AAV Cre in part because of its ability to mediate long-term gene expression changes. Given that Experiment 3 utilized our longest intervention period to date, we first confirmed decreased liver mRNA expression of ESR1 in both IM and MAT LERKO mice compared to control animals matched by maturity status ($P < .01$; Fig. 5A). In this experiment we were also able to detect hepatic mRNA expression of ESR2 above threshold levels for 5 CON and 6 LERKO animals in the

immature cohort only and found no difference by genotype (Fig. 5B). In contrast to what we found in Experiment 1, here we report no significant differences in liver whole homogenate protein expression of ER α by genotype (Fig. 5C).

Experiment 3. Hepatic Mitochondrial Respiration, H₂O₂ Flux, Coupling, and OXPHOS Protein Are Unchanged With Loss of Liver ER α

We measured O₂ and H₂O₂ flux simultaneously using high-resolution respirometry and calculated the coupling control ratio (Basal/State 3 [ADP-stimulated] respiration) to infer mitochondrial coupling. Neither pyruvate (PGM) nor palmitoyl-CoA (PCoA) supported respiration were different between CON and LERKO mice at any respiration state (Basal, State3, State3S, Uncoupled) in either the sexually immature or mature

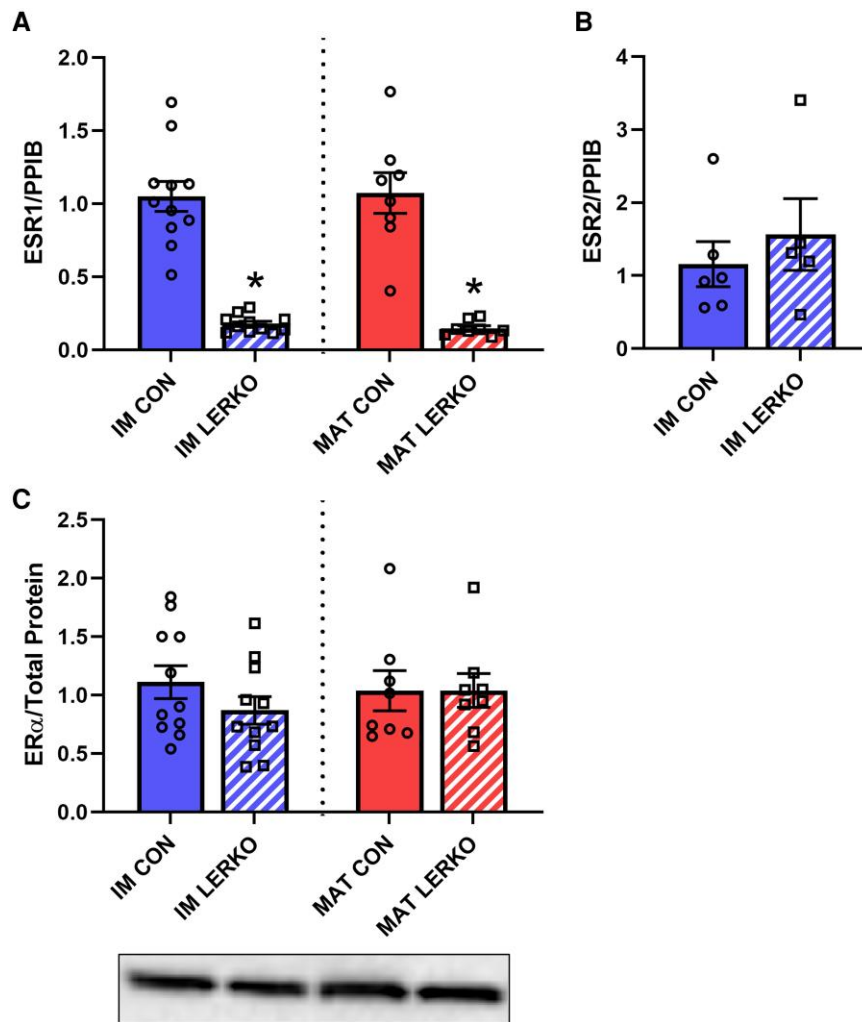


Figure 5. IM and MAT LERKO animals present with lower ESR1 mRNA gene expression but unaltered ER α protein expression. Liver mRNA expression of ESR1 and ESR2 was measured with RT-PCR (A, B). Protein expression of ER α was determined via Western blotting and normalized to total protein using amido black staining (C). A representative immunoblot is shown below the graph with the same load order (IM CON, IM LERKO, MAT CON, MAT LERKO). Data are presented as mean \pm SEM; n = 8-11 per group with only n = 5-6 for panel B. All mice were fed a chronic high-fat diet (8 weeks) and singly housed at thermoneutral. *denotes a significant difference ($P < .01$) compared with control animals within maturity status.

animals (Fig. 6A and 6D). Similarly, there was no difference by genotype in H₂O₂ emission across respiratory states (Fig. 6B and 6E). Liver mitochondrial coupling was also similar between LERKO and CON animals across both substrates and timing of genotype induction (Fig. 6C and 6F).

To further evaluate and phenotype liver mitochondria in LERKO mice induced pre and post sexual maturity, we evaluated whole homogenate OXPHOS protein expression, the protein complexes responsible for coupling oxidation of reducing equivalents to proton pumping eventually used as a gradient to synthesize ATP. There was no difference in OXPHOS protein expression between CON and LERKO mice in either induction maturity group (Fig. 6G).

Experiment 3. LERKO Animals Do Not Develop Steatosis and Maintain Antioxidant Signaling in the Liver

Ovariectomy studies suggest that female protection against hepatic steatosis and associated liver injury is regulated by estrogen action [8]. Therefore, we aimed to evaluate whether

LERKO, induced in sexually immature or mature mice, presented alterations in liver health. Liver triglycerides, a measure of hepatic steatosis, was quantified via biochemical assay and we found no changes between CON and LERKO mice in either cohort (Fig. 7A). Lipid peroxidation is a common feature of NAFLD, which results from reactive oxygen species interacting with polyunsaturated fatty acids. 4-Hydroxynonenal (4HNE) is a highly reactive product of lipid peroxidation which can freely diffuse in the extracellular space and amplify detrimental effects of oxidative stress [37]. We measured 4HNE protein expression in hepatic whole homogenates and saw no differences in the LERKO mice compared with controls (Fig. 7B).

Experiment 3. RNA Sequencing Reveals Greater Gene Expression Differences in Immature LERKO Mice

As an exploratory analysis, gene expression profiling of liver samples from mature and immature LERKO and CON mice was carried out using mRNA-sequencing. Principal

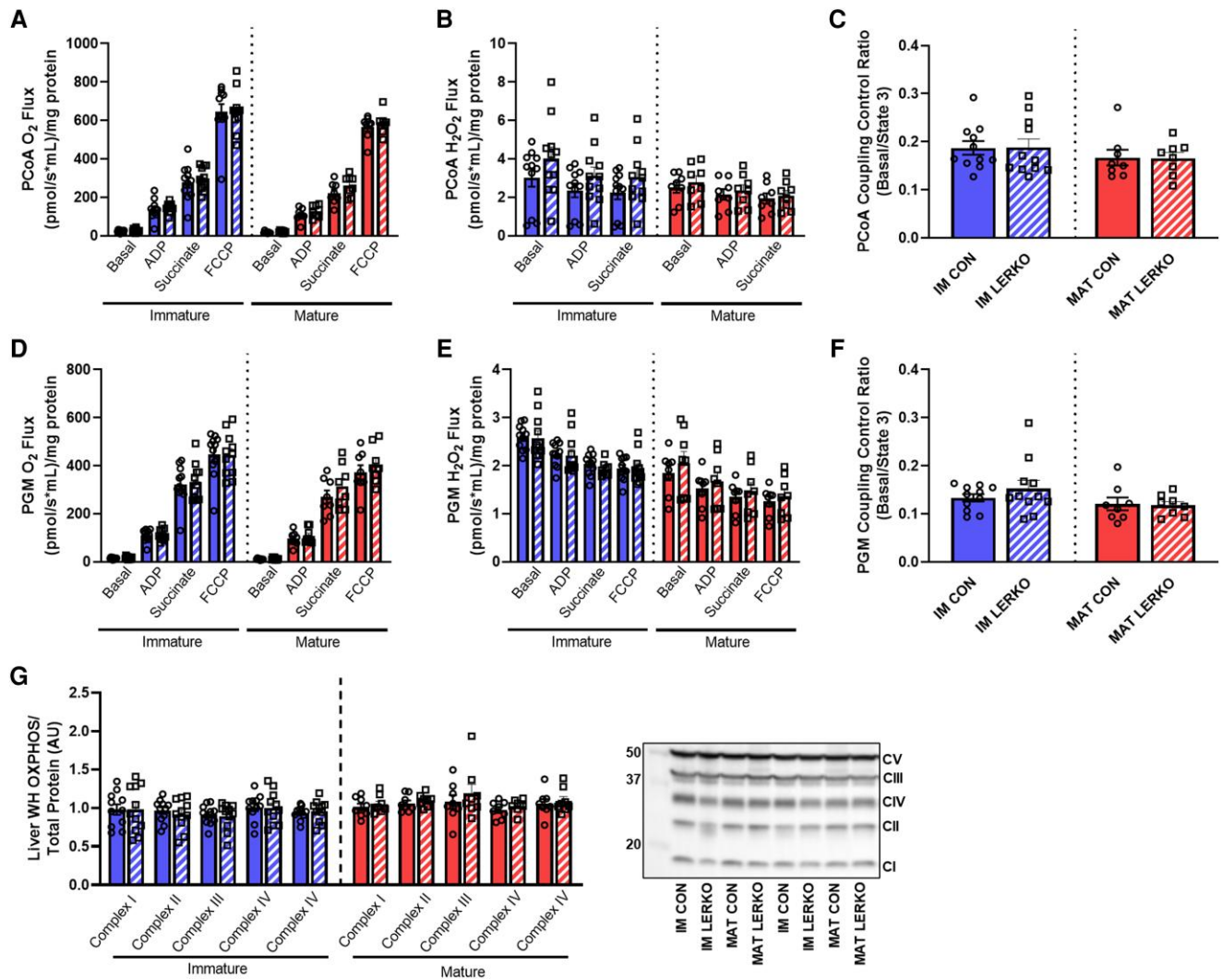


Figure 6. Hepatic mitochondrial respiration, H₂O₂, coupling, and OXPHOS protein were similar between CON and LERKO mice. Hepatic mitochondrial O₂ and H₂O₂ flux were measured with an Oxygraph O2k-Fluorometer under lipid (PCoA; A, B) and carbohydrate (PGM; D, E) substrate conditions. The coupling control ratio was calculated as basal respiration divided by ADP-stimulated (State 3) respiration (C, F). Liver whole homogenate oxidative phosphorylate complex protein expression was determined via Western blotting and normalized to the total protein via amido black staining (G). A representative immunoblot is included. Statistical differences across mitochondrial respiratory states were not determined. Data are presented as mean \pm SEM; n = 8-11 per group; all mice were fed a chronic high-fat diet (8 weeks) and singly housed at thermoneutral.

components analysis of all expressed genes indicated that global profiles of genes were more variable in immature LERKO (relative to CON) compared to mature mice (Fig. 8A). Comparisons between LERKO and CON mice showed 121 differentially expressed genes (DEGs) in immature and 485 DEGs in mature mice (Fig. 8B). The top 20 differentially expressed genes in mature LERKO mice are plotted in Fig. 8C and include genes for several isoforms of cytochrome P450 and sulfotransferases, which show a striking increase in mature LERKO mice. Analysis of DEGs in mature animals also showed enrichment of genes related to extracellular matrix, hormone stimulus, and insulin signaling (Fig. 8D). Tissue-specific network analysis of these genes using the HumanBase functional module enrichment revealed that among genes influenced by LERKO loss in mature mice, biological processes related to extracellular matrix, carbohydrate metabolism, and lipid biosynthesis were significantly enriched. Using Ingenuity Pathway Analysis software, we further analyzed function, pathways, and upstream regulators

among DEGs in mature LERKO (Fig. 8E). Functions related to synthesis and metabolism, apoptosis, fibrosis, and inflammatory response were altered in mature LERKO mice. Pathways related to hepatic cholestasis, stellate cell activation, and insulin signaling, along with regulators implicated in these processes (ESR2, PPAR γ , INSR) were significantly enriched among mature LERKO mice (Fig. 8E and 8F). Finally, we also directly contrasted altered functions, regulators, and pathways following LERKO loss between mature and immature mice (Fig. 8E and 8F). Akin to DEGs, signatures of LERKO loss were highly influenced by sexual maturation stage. Broadly, while fibrogenesis, extracellular matrix homeostasis and apoptosis were affected in mature mice, immature mice showed changes in mitochondria, reactive oxygen species (ROS) metabolism, and lipid and triglyceride metabolism (Fig. 8F). Consistent with these differences, immature LERKO mice also showed predicted regulation via increased inflammation and cell cycle and lower insulin signaling (Fig. 8F; red up, blue down, black cannot predict).

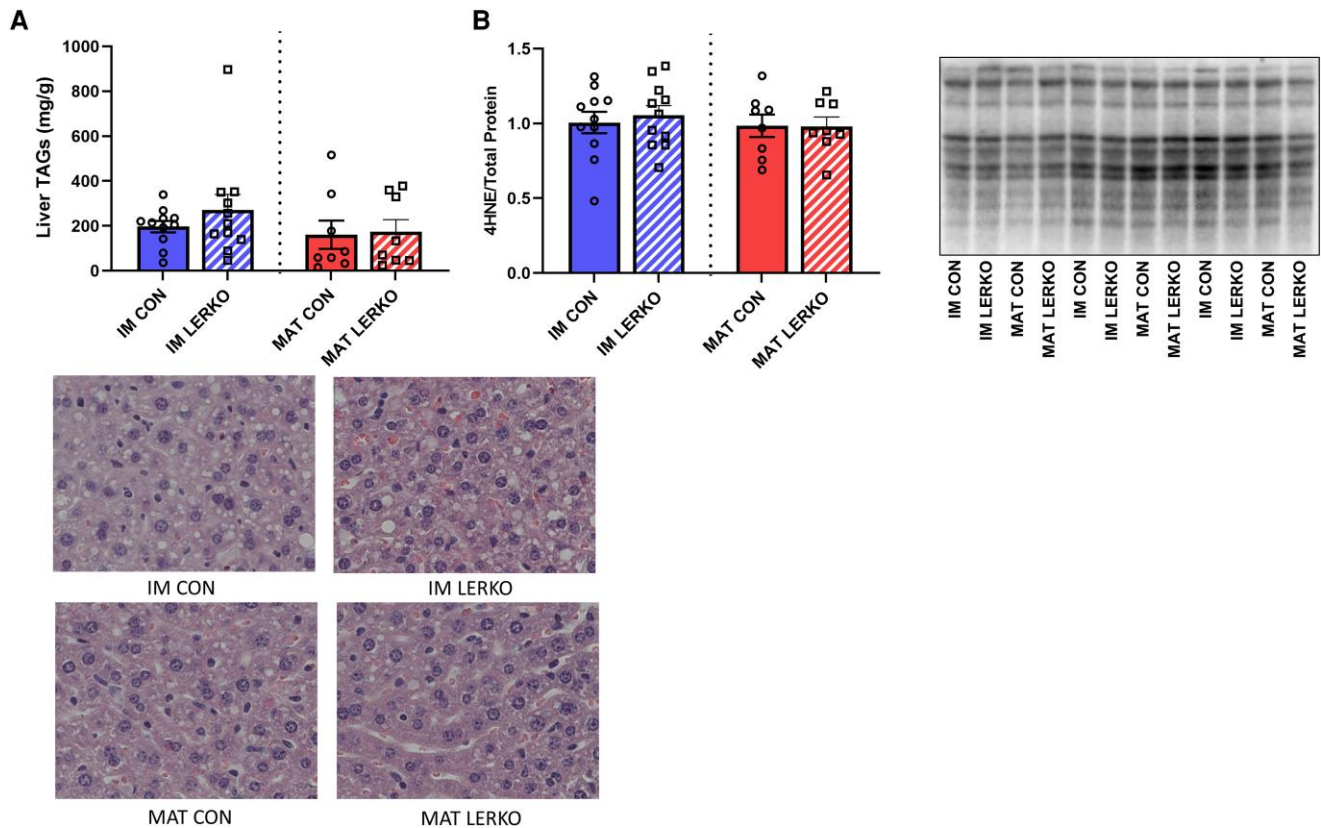


Figure 7. LERKO animals do not develop hepatic steatosis or liver injury. Hepatic steatosis (liver triglyceride content) was measured via biochemical assay (A). Protein expression of 4HNE, a lipid peroxidation product, was determined in whole liver homogenates via Western blotting and normalized to total protein using amido black staining (B). A representative immunoblot is shown to the right of the graph. H&E images of the liver from each group (C). Data are presented as mean \pm SEM; $n = 8-11$ per group; all mice were fed a chronic high-fat diet (8 weeks) and singly housed at thermoneutral.

Since LERKO significantly impacted insulin response and metabolic processes, we specifically queried genes related to related gene ontology (GO) biological processes (regulation of OXPHOS; bile acid metabolism; and lipid homeostasis). These analyses indicate significant alterations in key genes including altered expression of *Lipin2*, *Trib3*, *Tgfb1*, *Cpt1b*, and *Lipg* in mature LERKO mice (Fig. 9A-9C).

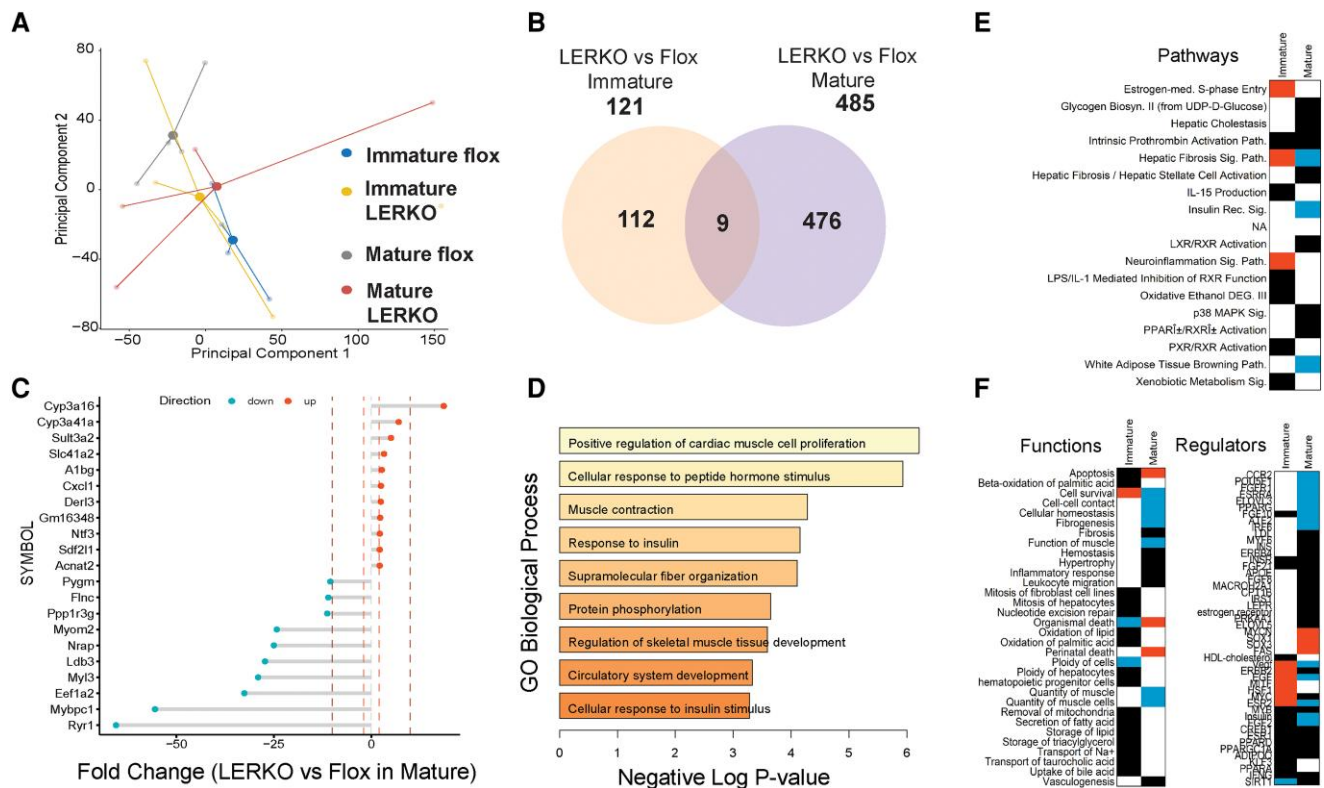
Experiment 3. LERKO Animals Have Similar Total Bile Acids, but Differ From Controls in Certain Bile Acid Species

To further explore changes in bile acid homeostasis, we quantified hepatic bile acids. First, we measured total hepatic bile acid concentrations and report similar levels between CON and LERKO mice within both MAT and IMM cohorts (Fig. 10A). Bile acids have unique metabolic signaling properties and physiological functions [38], and therefore we next evaluated the concentrations of individual bile acid species by LERKO status (Fig. 10B and 10C). Compared to their CON counterparts, both IMM and MAT LERKO mice had significantly lower cholic acid (CA), while tauroolithocholic acid (T-LCA) was only reduced in the LERKO mice induced at sexual immaturity (both $P < .05$; Fig. 10B). All other bile acid species measured (chenodeoxycholic acid [CDCA]; deoxycholic acid [DCA]; tauroolithocholic acid [T-LCA]; α -muricholic acid [α MCA]; β -muricholic acid [β MCA]; ω -muricholic acid [ω MCA]; tauro-chenodeoxycholic acid [T-CDCA]; tauro-deoxycholic acid [T-DCA]; tauro-

hyodexycolic acid [T-HDCA]; tauro-ursodeoxycholate [T-UDCA]; tauro ω -muricholic [T- ω MCA]) were similar across genotypes.

Discussion

We investigated the effects of an inducible reduction of hepatic ER α in combination with a short-term or chronic HFD on liver mitochondrial health and susceptibility to hepatic steatosis. We also tested if timing of LERKO induction, whether it be prior to or at sexual maturity (post estrogen surge), would alter these responses or impact hepatic transcriptional changes. Our original hypotheses were that LERKO mice would exhibit impaired hepatic mitochondrial respiratory capacity, greater H₂O₂ emission, and higher susceptibility to steatosis compared with control mice. We further expected that the induced reduction of hepatic ER α at sexual immaturity would exacerbate this phenotype compared with induction at sexual maturity. In contrast with these hypotheses, we report novel findings that ablation of ER α in liver does not alter susceptibility to hepatic steatosis or differences in mitochondrial outcomes under these dietary conditions, suggesting that full hepatic ER α expression is not required for regulation of these processes in female mice. In addition, our data suggest that while timing of ER α reduction did not significantly impact hepatic mitochondrial respiratory measures, there were large changes in hepatic gene expression of metabolic pathways measured by RNA sequencing.



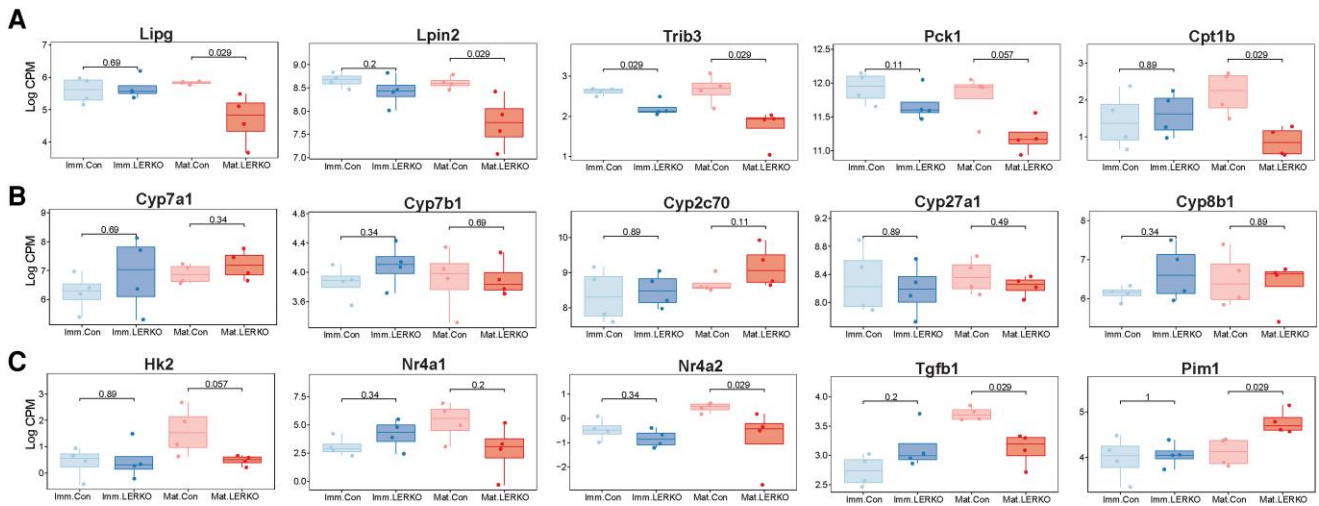


Figure 9. Hepatic mRNA expression of specific targets in mature and immature LERKO mice. mRNA expression of select cholesterol, bile acid, and mitochondrial OXPHOS genes. Normalized expression of select (A) lipid metabolism genes (Lipg, Lpin2, Trib3, Pck1, Cpt1b), (B) cholesterol metabolism (Cyp7a1, Cyp7b1, Cyp2c70, Cyp27a1, Cyp8b1) (C) regulators of metabolism and fibrosis (Hk2, Nr4a1, Nr4a2, Tgfb1, Pim1). Data are presented as boxplots; n = 4 per group; all mice were fed a chronic high-fat diet (8 weeks) and singly housed at thermoneutral. P values indicate comparisons between LERKO and flox groups.

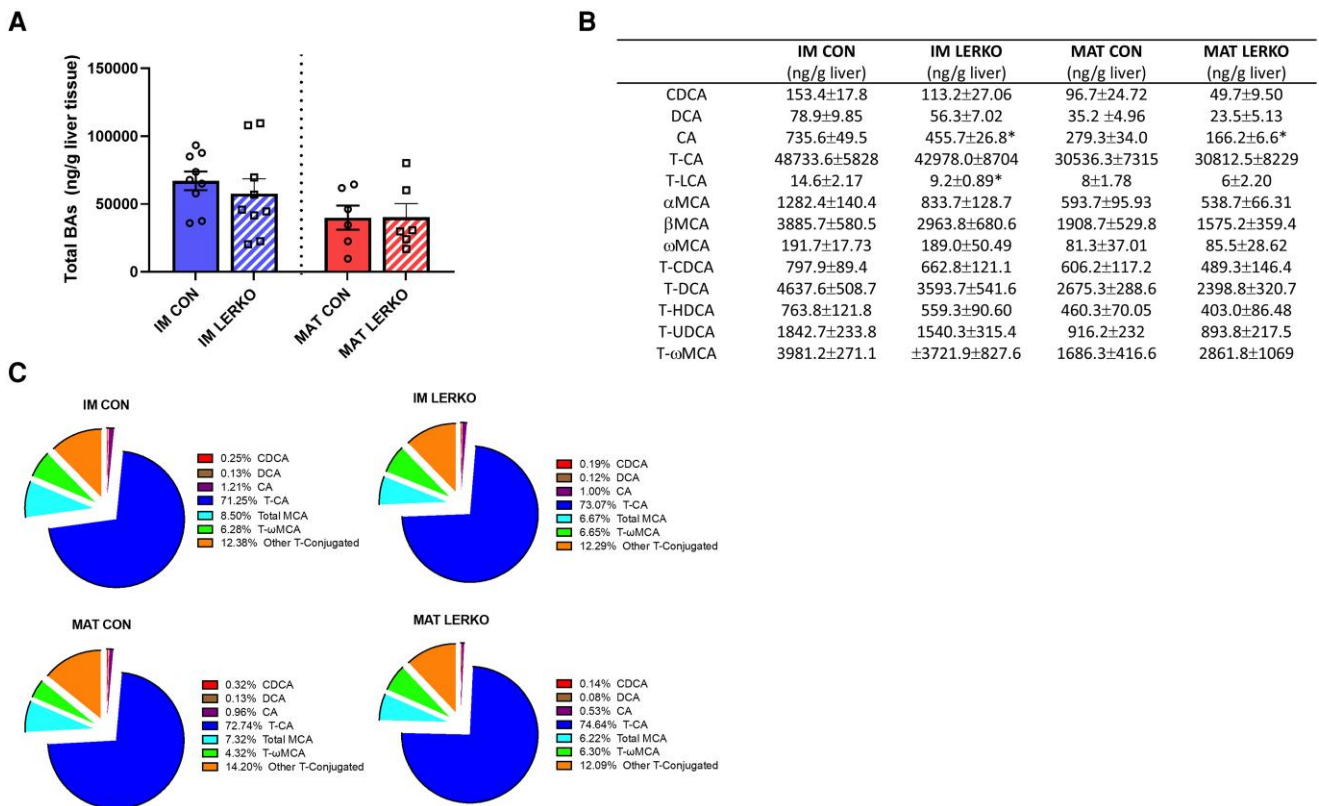


Figure 10. Specific bile acid (BA) species, rather than the total bile acid pool, are altered in LERKO mice. Total bile acid concentration measured by LC-MS. (A) Total BA concentrations. (B) Table showing the concentration of individual bile acid species. (C) Pie chart showing the percent of the total BA pool comprised of each bile acid species: chenodeoxycholic acid (CDC); deoxycholic acid (DCA); cholic acid (CA); tauro-cholic acid (T-CA); tauro-lithocholic acid (T-LCA); alpha-muricholic acid (αMCA); β-muricholic acid (βMCA); ω-muricholic acid (ωMCA); tauro-chenodeoxycholic acid (T-CDCA); tauro-deoxycholic acid (T-DCA); tauro-hydroxycholic acid (T-HDCA); tauro-ursodeoxycholate (T-UDCA); and tauro-ω-muricholic (T- ωMCA). Data are presented as mean ± SEM; n = 6-11 per group; all mice were fed an acute high-fat diet (4 weeks) and singly housed at thermoneutral; *denotes a significant difference (P < .05) compared with control animals within maturity status.

estradiol to prevent steatosis in LERKO mice following ovariectomy [8, 28]. In addition, a consistent finding between our present study and previous work is that LERKO mice have

similar body weight, fat mass, and serum triglycerides as control mice on a control or an HFD [27, 28, 45]. Given that these metabolic health markers are impacted by the loss of

estrogen-induced via ovariectomy [12], these data suggest that the mechanisms are likely due to extrahepatic ER α or the activity of other estrogen receptors.

To our knowledge, this is the first study to investigate if the timing of liver-specific ER α reduction at 2 different developmental periods in sex hormone biology (4 weeks of age marking sexually immature and 8-10 weeks of age representing sexual maturity) provide unique insights into the effects of LERKO loss under these developmentally distinct conditions. Transcriptomic analysis of the liver clearly showed that LERKO loss leads to widely different effects on hepatic gene expression and that changes are dependent on the developmental stage. While we did not examine the time of induction as a statistical analysis for comparison, we were able to evaluate whether LERKO mice differed from their respective controls in one or both maturity cohorts. This question is important considering that pre- and peri-pubertal girls experience surges in serum hormone concentrations that precede development of secondary sex characteristics [46]. Much like the transition to menopause (the cessation of sex hormone production) the onset and surge of estradiol production at puberty signals robust physiological and metabolic changes, including but not limited to reactivation of the hypothalamic-pituitary-gonadal axis and increased growth hormone production, both of which are known contributors to energy homeostasis and metabolic health [47]. More recently appreciated is that the timing of puberty onset is sensitive to nutrition and metabolic status and that there are several metabolic modulators of puberty (mTOR, AMPK, SIRT1) [48–50]. Contrary to our hypothesis of exacerbated steatosis and suboptimal hepatic mitochondrial function in LERKO mice induced before sexual maturity, we did not find divergent phenotypes between LERKO induction in sexually immature vs sexual maturity mice, suggesting that ER α does not mediate a priming/protective effect of pubertal estrogen surge on hepatic health or mitochondrial function. While NAFLD is rather uncommon in premenopausal women, there is a high prevalence of steatosis in adolescents and women with polycystic ovary syndrome, an endocrine disorder characterized by hyperandrogenism and ovulatory dysfunction [51]. Especially given the rise of obesity and sedentary behavior among adolescents (risk factors for NAFLD), it is critical to gain understanding of how estrogen action prior to and at puberty, as well as with endocrine disorders, modulates steatosis risk. Just like in menopause, studying the unique physiological changes at menarche is likely to be vital to our understanding of estrogen action in metabolic tissues as well as possible metabolic programming that may occur in peripheral tissues during this stage.

Given the potent role of ER α to mediate the impact of estrogen signaling on transcriptional regulation in the liver, we also performed bulk RNA sequencing to determine if LERKO mice at either time point displayed different gene expression profiles. Overall, LERKO and CON mice showed a significant number of differentially expressed genes both in immature (121 genes) and mature (485 genes). However, these only passed unadjusted *P* values and should be considered exploratory. Ingenuity Pathway Analysis revealed LERKO impacted transcriptional regulation for the synthesis of cholesterol, lipids, and steroids. Importantly, the sexual maturation stage in which the ER α was reduced significantly impacted changes in gene expression profile. Genes controlling steroid, cholesterol,

and bile acid metabolism were affected in mature LERKO mice, but genes controlling mitochondria biology, ROS metabolism, and cell homeostasis (apoptosis, survival) were more altered in immature mice. These gene expression differences suggest that perhaps a longer duration of ER α knockout is required to see significant metabolic and mitochondrial changes or that there are compensatory pathways that maintain metabolic homeostasis following significant ER α reductions, adaptations that prevent metabolic phenotypes from emerging. Given the gene expression changes found for bile acid metabolism and our previous finding that OVX and estradiol replacement altered CYP7a1 hepatic gene expression [12], we also measured hepatic bile acid species. Our findings indicate no change in total hepatic bile acid levels or major changes in the percent of different species comprising the total bile acid pool. However, we did find that LERKO mice in both immature and mature conditions displayed a significant reduction in liver cholic acid concentration and that only the immature LERKO had a significant decrease in tauroolithocholic acid (T-LCA) although there was also a trend for this species to decrease in the mature LERKO as well. Cholic acid is one of two primary bile acids synthesized in the liver from cholesterol and thus a reduction in cholic acid could suggest overall lower bile acid synthesis; however, other primary bile acids (CDCA and MCA) were not significantly reduced in LERKO mice although there were strong trends for reductions, particularly for CDCA. Thus, more work is needed to determine if LERKO mice display differences in bile acid synthesis metabolism, including studies comparing liver and serum bile acid levels in postprandial to postabsorptive conditions, which would limit variability and test conditions when bile acid metabolism is modulated by nutrient conditions.

Understanding the underlying mechanisms of estrogen action on hepatic mitochondrial function and liver steatosis risk is essential for women's health, especially given that women are spending more years in the postmenopausal period. These experiments are novel and informative for several reasons: first, we utilized a conditional LERKO model to remove any confounding effects of the loss of estrogen during fetal development; second, we induced the LERKO genotype at 2 different developmental stages (sexual immaturity, sexual maturity) to capture potential protective effects of the pubertal estrogen surge; and third, we believe this is the first report focused on hepatic ER α and mitochondrial function. Despite these strengths, the present studies are not without limitations. We opted to utilize a high-fat diet in all our studies, but these experiments would be strengthened by the addition of a low-fat diet control group. In addition, male mice should be included for future comparisons.

To conclude, these data suggest that the estrogen-dependent sexual dimorphism in susceptibility to hepatic steatosis and liver mitochondrial respiration, ROS emission, and coupling is not dependent on hepatic ER α signaling and instead is due to extrahepatic effects (peripheral or centrally mediated) or those not specific to ER α . However, our findings do show that ER α deletion does significantly impact global hepatic gene expression, particularly for pathways that are known to be mediated by estrogen signaling, cholesterol, and bile acid synthesis. The LERKO-induced changes in hepatic gene expression were associated with modest differences in hepatic bile acid species content.

Funding

This work was supported by a VA Merit Review Grant (1I01BX002567-01: J.P.T.); American Heart Award Predoctoral Fellowship Grant (20PRE35120098: K.N.Z.F.); and NIH Grants (1S10OD028598-01: J.P.T.; P20 GM103418: J.P.T.; 5 P30DK048520-27: K.S.; R01HD102726-01: K.S.).

Disclosures

None of the authors have any conflicts of interest to disclose.

Data Availability

Original data generated and analyzed during this study are included in this published article or in the data repositories listed in References. Raw and processed RNA-seq data are available from the NCBI Gene Expression Omnibus under record GSE228773.

References

- Saeedi P, Petersohn I, Salpea P, *et al.* Global and regional diabetes prevalence estimates for 2019 and projections for 2030 and 2045: results from the international diabetes federation diabetes Atlas, 9(th) edition. *Diabetes Res Clin Pract.* 2019;157:107843.
- Hallajzadeh J, Khoramdad M, Izadi N, *et al.* Metabolic syndrome and its components in premenopausal and postmenopausal women: a comprehensive systematic review and meta-analysis on observational studies. *Menopause.* 2018;25(10):1155-1164.
- Matsuo K, Gualtieri MR, Cahoon SS, *et al.* Surgical menopause and increased risk of nonalcoholic fatty liver disease in endometrial cancer. *Menopause.* 2016;23(2):189-196.
- Hevener AL, Clegg DJ, Mauvais-Jarvis F. Impaired estrogen receptor action in the pathogenesis of the metabolic syndrome. *Mol Cell Endocrinol.* 2015;418 Pt 3(Pt 3):306-321.
- Chen Y, Huang Q, Ai P, *et al.* Association between serum uric acid and non-alcoholic fatty liver disease according to different menstrual status groups. *Can J Gastroenterol Hepatol.* 2019;2019:2763093.
- Gutierrez-Grobe Y, Ponciano-Rodríguez G, Ramos MH, Uribe M, Méndez-Sánchez N. Prevalence of non alcoholic fatty liver disease in premenopausal, postmenopausal and polycystic ovary syndrome women. The role of estrogens. *Ann Hepatol.* 2010;9(4):402-409.
- McCain CS, Von Schulze A, Allen J, *et al.* Sex modulates hepatic mitochondrial adaptations to high-fat diet and physical activity. *Am J Physiol Endocrinol Metab.* 2019;317(2):E298-E311.
- Zhu L, Brown WC, Cai Q, *et al.* Estrogen treatment after ovariectomy protects against fatty liver and may improve pathway-selective insulin resistance. *Diabetes.* 2013;62(2):424-434.
- Younossi ZM, Stepanova M, Younossi Y, *et al.* Epidemiology of chronic liver diseases in the USA in the past three decades. *Gut.* 2020;69(3):564-568.
- Fuller KNZ, McCain CS, Allen J, *et al.* Sex and BNIP3 genotype, rather than acute lipid injection, modulate hepatic mitochondrial function and steatosis risk in mice. *J Appl Physiol (1985).* 2020;128(5):1251-1261.
- Von Schulze A, McCain CS, Onyekere C, *et al.* Hepatic mitochondrial adaptations to physical activity: impact of sexual dimorphism, PGC1alpha and BNIP3-mediated mitophagy. *J Physiol.* 2018;596(24):6157-6171.
- Fuller KNZ, McCain CS, Von Schulze AT, Houchen CJ, Choi MA, Thyfault JP. Estradiol treatment or modest exercise improves hepatic health and mitochondrial outcomes in female mice following ovariectomy. *Am J Physiol Endocrinol Metab.* 2021;320(6):E1020-E1031.
- Santamaria E, Avila MA, Latasa MU, *et al.* Functional proteomics of nonalcoholic steatohepatitis: mitochondrial proteins as targets of S-adenosylmethionine. *Proc Natl Acad Sci U S A.* 2003;100(6):3065-3070.
- Ibdah JA, Perlegas P, Zhao Y, *et al.* Mice heterozygous for a defect in mitochondrial trifunctional protein develop hepatic steatosis and insulin resistance. *Gastroenterology.* 2005;128(5):1381-1390.
- Rector RS, Thyfault JP, Uptergrove GM, *et al.* Mitochondrial dysfunction precedes insulin resistance and hepatic steatosis and contributes to the natural history of non-alcoholic fatty liver disease in an obese rodent model. *J Hepatol.* 2010;52(5):727-736.
- Sanyal AJ, Campbell-Sargent C, Mirshahi F, *et al.* Nonalcoholic steatohepatitis: association of insulin resistance and mitochondrial abnormalities. *Gastroenterology.* 2001;120(5):1183-1192.
- Perez-Carreras M, *et al.* Defective hepatic mitochondrial respiratory chain in patients with nonalcoholic steatohepatitis. *Hepatology.* 2003;38(4):999-1007.
- Koliaki C, Szendroedi J, Kaul K, *et al.* Adaptation of hepatic mitochondrial function in humans with non-alcoholic fatty liver is lost in steatohepatitis. *Cell Metab.* 2015;21(5):739-746.
- Gao H, Fält S, Sandelin A, Gustafsson JA, Dahlman-Wright K. Genome-wide identification of estrogen receptor alpha-binding sites in mouse liver. *Mol Endocrinol.* 2008;22(1):10-22.
- Hevener A, Reichart D, Janez A, Olefsky J. Female rats do not exhibit free fatty acid-induced insulin resistance. *Diabetes.* 2002;51(6):1907-1912.
- Clegg D, Hevener AL, Moreau KL, *et al.* Sex hormones and cardiometabolic health: role of estrogen and estrogen receptors. *Endocrinology.* 2017;158(5):1095-1105.
- Ribas V, Drew BG, Zhou Z, *et al.* Skeletal muscle action of estrogen receptor alpha is critical for the maintenance of mitochondrial function and metabolic homeostasis in females. *Sci Transl Med.* 2016;8(334):334ra54.
- Iñigo MR, Amorese AJ, Tarpey MD, *et al.* Estrogen receptor-alpha in female skeletal muscle is not required for regulation of muscle insulin sensitivity and mitochondrial regulation. *Mol Metab.* 2020;34:1-15.
- Prossnitz ER, Barton M. Estrogen biology: new insights into GPER function and clinical opportunities. *Mol Cell Endocrinol.* 2014;389(1-2):71-83.
- Sharma G, Prossnitz ER. G-Protein-Coupled Estrogen Receptor (GPER) and sex-specific metabolic homeostasis. *Adv Exp Med Biol.* 2017;1043:427-453.
- Mancino A, Mancino MG, Glaser SS, *et al.* Estrogens stimulate the proliferation of human cholangiocarcinoma by inducing the expression and secretion of vascular endothelial growth factor. *Dig Liver Dis.* 2009;41(2):156-163.
- Hart-Unger S, Arao Y, Hamilton KJ, *et al.* Hormone signaling and fatty liver in females: analysis of estrogen receptor alpha mutant mice. *Int J Obes (Lond).* 2017;41(6):945-954.
- Guillaume M, Riant E, Fabre A, *et al.* Selective liver estrogen receptor alpha modulation prevents steatosis, diabetes, and obesity through the anorectic growth differentiation factor 15 hepatokine in mice. *Hepatology Commun.* 2019;3(7):908-924.
- Albrecht ED, Pepe GJ. Estrogen regulation of placental angiogenesis and fetal ovarian development during primate pregnancy. *Int J Dev Biol.* 2010;54(2-3):397-408.
- Bidlingmaier F, Wagner-Barnack M, Butenandt O, Knorr D. Plasma estrogens in childhood and puberty under physiologic and pathologic conditions. *Pediatr Res.* 1973;7(11):901-907.
- Martin-Millan M, Almeida M, Ambrogini E, *et al.* The estrogen receptor-alpha in osteoclasts mediates the protective effects of estrogens on cancellous but not cortical bone. *Mol Endocrinol.* 2010;24(2):323-334.
- Pesta D, Gnaiger E. High-resolution respirometry: OXPHOS protocols for human cells and permeabilized fibers from small biopsies of human muscle. *Methods Mol Biol.* 2012;810:25-58.
- Law CW, Alhamdoosh M, Su S, *et al.* RNA-seq analysis is easy as 1-2-3 with limma, glimma and edgeR. *F1000Res.* 2016;5:ISCB Comm J-1408.

34. Kuleshov MV, Jones MR, Rouillard AD, *et al.* Enrichr: a comprehensive gene set enrichment analysis web server 2016 update. *Nucleic Acids Res.* 2016;44(W1):W90-W97.
35. Krishnan A, Zhang R, Yao V, *et al.* Genome-wide prediction and functional characterization of the genetic basis of autism spectrum disorder. *Nat Neurosci.* 2016;19(11):1454-1462.
36. Alnouti Y, Csanaky IL, Klaassen CD. Quantitative-profiling of bile acids and their conjugates in mouse liver, bile, plasma, and urine using LC-MS/MS. *J Chromatogr B Analyt Technol Biomed Life Sci.* 2008;873(2):209-217.
37. Ucar F, Sezer S, Erdogan S, Akyol S, Armutcu F, Akyol O. The relationship between oxidative stress and nonalcoholic fatty liver disease: its effects on the development of nonalcoholic steatohepatitis. *Redox Rep.* 2013;18(4):127-133.
38. de Boer JF, Bloks VW, Verkade E, Heiner-Fokkema MR, Kuipers F. New insights in the multiple roles of bile acids and their signaling pathways in metabolic control. *Curr Opin Lipidol.* 2018;29(3):194-202.
39. Zhou Y, Shimizu I, Lu G, *et al.* Hepatic stellate cells contain the functional estrogen receptor beta but not the estrogen receptor alpha in male and female rats. *Biochem Biophys Res Commun.* 2001;286(5):1059-1065.
40. Shimizu T, Suzuki T, Yu HP, *et al.* The role of estrogen receptor subtypes on hepatic neutrophil accumulation following trauma-hemorrhage: direct modulation of CINC-1 production by Kupffer cells. *Cytokine.* 2008;43(1):88-92.
41. Vickers AE, Lucier GW. Estrogen receptor levels and occupancy in hepatic sinusoidal endothelial and Kupffer cells are enhanced by initiation with diethylnitrosamine and promotion with 17alpha-ethinylestradiol in rats. *Carcinogenesis.* 1996;17(6):1235-1242.
42. Foryst-Ludwig A, Clemenz M, Hohmann S, *et al.* Metabolic actions of estrogen receptor beta (ERbeta) are mediated by a negative cross-talk with PPARgamma. *PLoS Genet.* 2008;4(6):e1000108.
43. Winn NC, Acin-Perez R, Woodford ML, *et al.* A thermogenic-like brown adipose tissue phenotype is dispensable for enhanced glucose tolerance in female mice. *Diabetes.* 2019;68(9):1717-1729.
44. Meoli L, Isensee J, Zazzu V, *et al.* Sex- and age-dependent effects of Gpr30 genetic deletion on the metabolic and cardiovascular profiles of diet-induced obese mice. *Gene.* 2014;540(2):210-216.
45. Meda C, Barone M, Mitro N, *et al.* Hepatic ERalpha accounts for sex differences in the ability to cope with an excess of dietary lipids. *Mol Metab.* 2020;32:97-108.
46. Biro FM, Pinney SM, Huang B, Baker ER, Walt Chandler D, Dorn LD. Hormone changes in peripubertal girls. *J Clin Endocrinol Metab.* 2014;99(10):3829-3835.
47. Mohr MA, Wong AM, Tomm RJ, Soma KK, Micevych PE. Pubertal development of estradiol-induced hypothalamic progesterone synthesis. *Horm Behav.* 2019;111:110-113.
48. Martos-Moreno GA, Chowen JA, Argente J. Metabolic signals in human puberty: effects of over and undernutrition. *Mol Cell Endocrinol.* 2010;324(1-2):70-81.
49. Sánchez-Garrido MA, Castellano JM, Ruiz-Pino F, *et al.* Metabolic programming of puberty: sexually dimorphic responses to early nutritional challenges. *Endocrinology.* 2013;154(9):3387-3400.
50. Vazquez MJ, Velasco I, Tena-Sempere M. Novel mechanisms for the metabolic control of puberty: implications for pubertal alterations in early-onset obesity and malnutrition. *J Endocrinol.* 2019;242(2):R51-R65.
51. Vassilatou E. Nonalcoholic fatty liver disease and polycystic ovary syndrome. *World J Gastroenterol.* 2014;20(26):8351-8363.